Microfabrication of Individual 200 μm Diameter Transdermal Microconduits Using High Voltage Pulsing in Salicylic Acid and Benzoic Acid

Ljubomir Ilic, T. R. Gowrishankar, Timothy E. Vaughan, Terry O. Herndon,* and James C. Weaver

Harvard-MIT Health Science and Technology, Massachusetts Institute of Technology, Cambridge, Massachusetts, U.S.A.; *MIT Lincoln Laboratories, Lexington, Massachusetts, U.S.A.

We describe an extension of semiconductor fabrication methods that creates individual ≈200 μm diameter aqueous pathways through human stratum corneum at predetermined sites. Our hypothesis is that spatially localized electroporation of the multilamellar lipid bilayer membranes provides rapid delivery of salicylic acid to the keratin within corneocytes, leading to localized keratin disruption and then to a microconduit. A microconduit penetrating the isolated stratum corneum supports a volumetric flow of order 0.01 ml per s with a pressure difference of only 0.01 atm (about 10^2 Pa). This study provides a method for rapidly microengineering a pathway in the skin to interface future devices for transdermal drug delivery and sampling of biologically relevant fluids. ***Key words: keratolytic agents/skin electroporation/stratum corneum/transdermal drug delivery. J Invest Dermatol 116:40–49, 2001***

Drug delivery continues to be of great and growing interest (Langer, 1998). Established delivery methods involving oral and injectable routes encounter significant problems, such as high first-pass hepatic metabolism and patient compliance. Minimally invasive transdermal intervention can avoid these problems and is increasingly viewed as an attractive alternative (Smith and Maibach, 1995; Guy, 1996; Schaefer and Redelmeier, 1996; Merino *et al*, 1997). Analyte extraction through the skin is also being considered as a mean for analyte sampling (Tamada *et al*, 1995; Smith *et al*, 1999; Kost *et al*, 2000). Transdermal molecular transport with temporal control would be valuable for both drug delivery and analyte sensing; however, the practical handling and obtrusiveness of present invasive transdermal delivery systems severely restrict their use in many day to day applications (Wouters and Dinh, 1997). Miniature devices that interface with the skin over a microscopic area would offer a desirable alternative for transdermal drug delivery and sampling. The stratum corneum (SC) of the skin, the main barrier to transdermal delivery, limits the transport to clinically insufficient rates for most biologically active macromolecules, such as insulin or heparin. In this study, we describe an electrochemical method to create a microconduit (a microscopic aqueous pathway extending through the thickness of the SC) in the skin that should facilitate an unhindered transport across the skin of any macromolecule.

Several types of physical interventions using ultrasound, laser, high pressure, and microfabrication have been attempted for altering the SC. Low-frequency ultrasound was shown to increase the permeability of human skin by several orders of magnitude to many drugs, including high molecular weight proteins (Mitragotri *et al*, 1995; Kost *et al*, 2000). Application of 168 kHz continuous ultrasound of spatially averaged pressure amplitude of 1.9×10^5 Pa generated defects in human SC specimens (Wu *et al*, 1998). A mid-infrared Er:YSGG laser was used to ablate cadaveric swine SC leading to an increased permeability for H-3-hydrocortisone (Nelson *et al*, 1991). A stress pulse generated by a single laser pulse was shown to increase transiently the permeability of the SC *in vivo* with recovery occurring within minutes (Lee *et al*, 1998). A device that uses compressed helium gas to accelerate microscopic particles into the skin was used as a delivery system for DNA vaccines to elicit a virus-specific response in mice (Degano *et al*, 1998). Silicon-processed microneedles have been shown to increase permeability of human skin *in vitro* (Henry *et al*, 1998; Lin and Pisano, 1999). Altea's MicroPor uses thermal energy to vaporize the top layer of the epidermis within a small, sharply defined region to deliver drugs (Eppstein *et al*, 1999) and sample interstitial fluid (Smith *et al*, 1999). Skin electroporation by high voltage pulsing provides an alternative method for transdermal drug delivery and analyte sampling. In this study, we report the creation of a microconduit at a known site in the SC by high-voltage pulsing in the presence of a keratolytic agent.

Skin electroporation is an extension of lipid bilayer membrane electroporation (Weaver and Chizmadzhev, 1996), in which a brief elevation of the transmembrane voltage is hypothesized to create aqueous pathways (**Fig 1**, center) across the multilamellar bilayer membranes of the SC (Weaver *et al*, 1999a,b). Based on the idea that electroporation could introduce low-toxicity keratolytic molecules into the corneocytes through these aqueous pathways, a hypothesis to create microconduits across SC was developed earlier (Ilic *et al*, 1999; Weaver *et al*, 1999b; Zewert *et al*, 1999). The combination of new aqueous pathways through the multilamellar lipid bilayer membranes and disruption of the keratin matrix could result in dislodgement of entire stacks of corneocytes (**Fig 1**, right), creating a minimum size (≈50 μm diameter) microconduit through the SC. Such an opening would present negligible steric hindrance to macromolecule transport. By using temporally controlled pressure-

Manuscript received February 11, 2000; revised October 13, 2000; accepted for publication October 17, 2000.

Reprint requests to: James C. Weaver, Harvard-MIT Health Science and Technology, Massachusetts Institute of Technology, Cambridge, MA 02139. Email: jim@hstbme.mit.edu

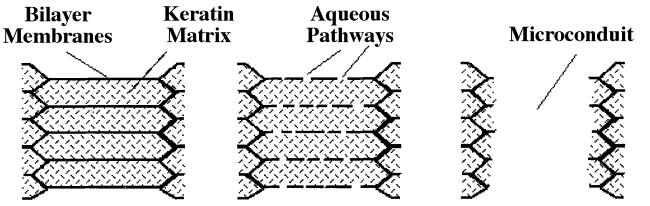

Figure 1. Illustration of the hypothesis of microconduit creation using a modified "brick wall model" for human SC. (Weaver *et al*, 1997, 1998) A single local transport region is depicted, showing only about one-third of the 15–16 corneocyte layers of the SC. For simplicity, ordered stacks (columns) of corneocytes (Menton, 1976) are shown. Similar behavior is expected with disordered (offset) columns (Bergstresser and Chapman, 1980), because typical corneocyte offsets introduce additional tortuosity that is about the same as the slight internal tortuosity expected within an ordered stack. Some of the pathways created by pulsing alone are hypothesized to be larger than pathways through the unperturbed keratin matrix (Zewert *et al*, 1995). *Left*: Site prior to aqueous pathway creation. *Left center*: Site after several high-voltage pulses, depicting a high area density of straight-through primary pathways within the local transport region before enlargement by introduction of keratolytic molecules. *Right*: Microconduit resulting from removal of most of a weakened stack of corneocytes after keratin matrix disruption.

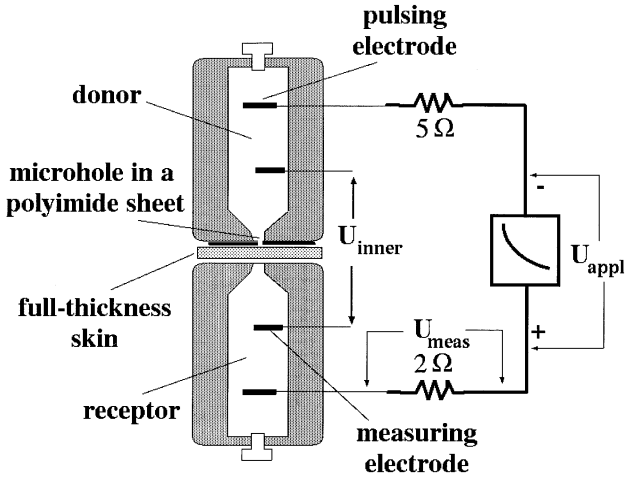

Figure 2. Chamber and circuitry used for electrochemical intervention. Both pulsing and measuring electrodes were made of stainless steel and were 3 cm long. The full-thickness skin was mounted with the SC contacting the 50 μm thick polyimide sheet containing a 200 μm diameter microhole. The current through the skin was determined from the voltage across the 2 Ω resistor. In all the experiments, the receptor compartment contained PBS (pH 7.4).

driven flow, large rates of molecular transport should be achieved, for both conventional pharmaceuticals and the larger peptides, proteins, and nucleotides from biotechnology.

Initial experiments (Zewert *et al*, 1999) using sodium thiosulfate (STS) as the keratolytic agent showed that a macromolecule (lactalbumin, ≈ 15,000 g per mol) and smaller, charged molecule (sulforhodamine, 600 g per mol) were transported at almost the same rate across heat-stripped human skin *in vitro*; however, a large variability in microconduit creation was observed. In a subsequent study, urea was added to stabilize the STS-reduced (broken) disulfide bridges reduced, preventing them from reforming by oxidation (Ilic *et al*, 1999). It was shown that ≈ 1200 mm^2 diameter microconduit spanning the SC was created following treatment with STS and urea. The microconduit was shown to support volumetric flow of order 0.01 ml per s by a pressure difference of only 0.01 atm (about 10^2 Pa), demonstrating that the SC barrier had been completely removed within this microscopic area. Other studies showed that electroporation could be constrained to occur at predetermined sites (microholes in an insulating thin sheet) even with imperfect skin contact (Gowrishankar *et al*, 1999).

In this study, we investigate the use of active ingredients of Whitfield's solution in creating a microconduit in human skin *in vitro*. Whitfield's solution, with established keratolytic properties, finds extensive use in the topical treatment of intractable, superficial (limited to the SC) dermatophyte infections of the skin (Holti, 1970; Clayton and Connor, 1973; Wright and Robertson, 1986; Russell and Russell, 1992; Gooskens *et al*, 1994; Diehl, 1996; Bennett, 1998). Whitfield's solution achieves chemical decomposition of keratin by breaking the keratin peptide bonds and by reducing the binding forces within the SC, which is likely the basis for its keratolytic mode of action (Huber and Christopher, 1977; Gloor and Beier, 1984; Nook, 1987; Neubert *et al*, 1990; Lóden *et al*, 1995; Budavari, 1996; Lin and Nakatsui, 1998). In this study we report a rapid, controlled method for creating a microconduit at a predetermined site in full-thickness human skin, with the microconduit supporting a pressure-driven flow across isolated SC.

MATERIALS AND METHODS

Microconduit creation procedure This *in vitro* study involves the investigation and partial optimization of an electrochemical process for microconduit creation. The two-step procedure involves:

1 Introduction of keratolytic chemicals into corneocytes at a predetermined microscopic area site by high-voltage pulsing that electroporates the multilamellar bilayer lipid membranes (Gowrishankar *et al*, 1999). This involves creation of many primary pores (diameter ≈ 1 nm) within a spatially constrained local transport region by using an electrically insulating mask with a single ≈ 200 μm microhole that spatially constrains the current; and

2 Rapid disruption of the keratin matrix within the electroporated corneocytes by the keratolytic solution.

Skin preparation Adult human skin was secured from the abdomen, arm, or back of cadavers (NDRI, Philadelphia, PA and Ohio Valley Tissue and Skin Center, Cincinnati, OH). The skin, stored at –70°C, was cut into 1 inch (2.54 cm) square pieces and thawed to room temperature prior to the start of the experiment. The microconduit creation step was carried out using full thickness skin. The flow test (see section on tests for microconduit presence below) was carried out on thinned skin, prepared by heat stripping and/or treated with trypsin.

Heat stripping yields a specimen of thickness 100 ± 50 μm. This procedure involves a well established method of immersing the skin in ≈ 60°C water for 2 min (Gummer, 1989). In some cases, overnight removal of the remaining epithelium was achieved by enzymatic trypsin digestion (Anderson *et al*, 1988). The heat-stripped skin was digested in 1% trypsin (Sigma, St Louis, MO, T-0134) for 12 h at 4°C.

Experimental chambers Both high-voltage pulsing during the microconduit creation phase and iontophoresis thereafter, were carried out in the top–bottom chamber of **Fig 2**. The chamber is a modified version of the side-by-side chamber in which the donor compartment is masked by a nonconducting polyimide sheet with an approximately 200 nm diameter microhole. A full-thickness skin specimen was mounted between the two compartments with the SC facing the donor and contacting the polyimide sheet. The flow test following the creation of a microconduit (after the skin was thinned) was performed in the side-by-side chamber of **Fig 3**.

Electrical pulsing In this study, the total time of the experiment, t_{total}, the interval between pulses, t_{int}, the high-voltage pulse decay constant, t_{pulse}, and the peak current, I, were selected to deliver a total charge of about 40 mC during the pulsing protocol. The voltage across the skin, U_{skin}, and the total charge transferred, q, were calculated according to Eq 1, and Eq 2, respectively.

$$U_{skin} = U_{inner} - R_{PBS}I = U_{inner} - R_{PBS}\frac{U_{meas}}{R_{meas}} \quad (1)$$

where R_{PBS} is the resistance of the phosphate-buffered saline (PBS) column between the measuring electrodes (**Fig 2**) with no skin present in the chamber. The peak voltage across the measuring electrodes, U_{inner}, and the peak current, I, were measured from the exponential waveforms recorded during high-voltage pulsing. For a measured peak current, I, the total number of coulombs, q, transferred over the total time is:

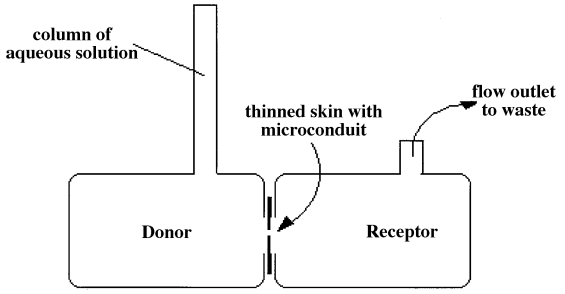

Figure 3. Chamber used in flow experiments. The electrochemically treated skin, after thinning by either heat stripping and/or treatment with trypsin, was mounted in the chamber with the SC facing the donor compartment. A column of aqueous solution was added to the donor compartment in order to establish a hydrostatic pressure difference across the skin. The presence of a microconduit in the skin resulted in a continuous decrease in the level of the aqueous column. The column height, h, was recorded at a number of time points and used in fluid flow analysis to estimate the diameter of the microconduit.

$$q = \frac{t_{total}}{t_{int}} \int_0^{\infty} I e^{-t'/\tau_{pulse}} dt' = \frac{t_{total}}{t_{int}} I \tau_{pulse} \qquad (2)$$

High-voltage pulses were applied using an exponential pulser (Electroporation System 600, BTX Industries, San Diego, CA). A noninductive, high power rating (25 W) resistor ($R_{meas} = 2\Omega$) was placed in series with the chamber in order to measure the current through the skin. The measuring electrodes consisted of stainless steel wires (0.7 mm diameter, 3 cm long) placed in the inner ports of the chamber parallel to skin surface, at a distance of 1.5 cm between them (**Fig 2**). The voltages across the inner electrodes (U_{inner}) and the 2 Ω series resistor during pulses ($U_{meas} = IR_{meas}$) were stored in a digital oscilloscope (Hewlett Packard 54601) for determining U_{skin} according to Eq 1.

Keratolytic molecules In this study, we used skin electroporation with a topically applied solution of keratolytic molecules: salicylic acid (Sigma, S-0875, 138 g per mol) and benzoic acid (Sigma, B-3250, 122 g per mol). In most experiments, 3% salicylic acid and 6% benzoic acid were used in a 70% ethanol and 30% PBS (pH 7.4) solution. These chemicals, in the concentrations mentioned above, form the active ingredients of Whitfield's solution, which is a well-established topical medication with keratolytic activity.

Fluorescent molecules Sulforhodamine (Sigma; 607 g per mol; z = –1; "red fluorescence"; 0.5 mM in donor compartment) was used as a fluorescent tracer, because it is both water soluble and sufficiently lipophylic that it also stains cell membranes (Chen *et al*, 1998), allowing tissue accessed by the microconduit to be stained. The sulforhodamine molecule size is about 1.5 nm, which allows it to be readily transported through the primary aqueous pathways (about 2 nm diameter) created by high-voltage pulsing, and to pass with negligible steric hindrance through the intact keratin matrix within corneocytes.

A 2.5% volume suspension of fluorescent latex beads (Fluoresbrite, "green fluorescence"; Polysciences, Warrington, PA; 1.5 μm diameter) with a large negative charge ($\approx -8 \times 10^{-12}$ C) was used. These microbeads are much larger than typical macromolecules, and can often be detected individually by fluorescence microscopy. Such beads do not penetrate the skin due to high-voltage pulsing alone (Chen *et al*, 1999), owing to both their large charge and size.

Positive control To assess microconduit creation, electrochemically treated full thickness skin specimens were first evaluated by four indicators that were established in positive control experiments. In these experiments, an approximately 200 μm diameter shallow microhole was drilled through the SC of a full thickness skin specimen by a cobalt microprecision drill bit (Gühring, Brookfield, WI). The skin specimen was then subjected to iontophoresis with PBS containing fluorescent markers in the donor side (contacting the SC). The rationale was that a small, constant current preferentially transports these negatively charged markers into the low resistance microhole, thereby marking it for optical microscopy.

Negative control Negative control experiments were performed on unperturbed full thickness skin. The skin specimen was mounted in the top–bottom chamber (**Fig 2**) with the donor compartment containing fluorescent markers in PBS. The skin was subjected to iontophoresis with the same electrical parameters as in an actual experiment involving electrochemical treatment.

Iontophoresis control Iontophoresis control experiments refer to direct (low-voltage) current treatment of full thickness skin in the presence of keratolytic molecules. The skin specimen was mounted in the top–bottom chamber (**Fig 2**) with the donor compartment containing 3% salicylic acid and 6% benzoic acid in 70% ethanol and 30% PBS solution. The skin was subjected to 1 mA per cm^2 (over the area of a microhole in the insulating sheet, i.e., $J = I/A_{\mu hole}$) iontophoresis for 1 h. Following the treatment, the donor solution was replaced with the fluorescent marker solution and the iontophoresis procedure was repeated for 1 h.

Pulsing control Pulsing control experiments relate to the electrical treatment of the skin without the use of keratolytic molecules. The skin was mounted in the top–bottom chamber (**Fig 2**) with the donor compartment containing PBS only, or 70% ethanol and 30% PBS. The skin was subjected to high-voltage pulsing and iontophoresis in the presence of fluorescent markers with the same electrical parameters as in an actual experiment involving electrochemical treatment with keratolytic molecules. Note that because the PBS solution has a lower electrical resistance than the 70% ethanol + 30% aqueous solution, a larger fraction of the applied voltage appears across the skin. The importance of this "variable voltage divider" effect is discussed elsewhere (Weaver *et al*, 1998; Pliquett 1999; Pliquett *et al*, 2000).

Experimental procedure The experimental procedure involved in the electrochemical creation of a microconduit and in the tests to confirm its presence is described below.

1 A previously thawed full-thickness human cadaver skin specimen was mounted in the top–bottom chamber (**Fig 2**), avoiding visible skin deformation by excessive pressure. The integrity of the skin was evaluated by measuring the initial skin electrical resistance between the pulsing electrodes.

2 In positive control experiments, a 200 μm microhole, approximately 40 ± 20 μm deep, was drilled in the skin. In negative control experiments, the skin was left unperturbed. In microconduit creation experiments, the donor compartment was filled with the keratolytic solution and the high-voltage pulsing protocol followed.

3 In order to transport negatively charged fluorescent markers electrically, 1 h of 1 mA per cm^2 iontophoresis was applied (over the region of the skin exposed to the microhole in the insulating sheet) with the donor containing the two fluorescent markers in PBS. The final skin resistance was measured following iontophoresis.

4 The skin was then examined by optical microscopy using both incandescent and fluorescent illumination. Further imaging and flow tests were performed after the skin was heat stripped, and in some cases, further treated with trypsin. Thus thinned skin was mounted in the side-by-side chamber (**Fig 3**) with a column of aqueous solution on the donor side. The flow was recorded at various time intervals as the decrease in the column level.

Tests for microconduit presence The creation of a microconduit was assessed using three independent tests: the resistance ratio test, the imaging tests, and the pressure-driven volumetric flow test. The first test was applied to full-thickness skin, the last test was applied after the skin was thinned by heat stripping (Gummer, 1989) or heat stripping and enzymatic (trypsin) digestion of the epidermis, the combination yielding isolated SC (Anderson *et al*, 1988). The second test was applied to both full-thickness and thinned skin specimens.

Resistance ratio test High-voltage pulsing and the use of keratolytic molecules create SC spanning aqueous pathways in the skin. This change in skin structure is reflected partially by a change in skin resistance. An LCR meter (SR715, Stanford Research Systems, Sunnyvale, CA) was used to measure the real part of the low frequency skin impedance (100 mV, 100 Hz sinusoidal input). A parallel RC model was assumed for the skin. Because the capacitance of the skin changes very little following high-voltage pulsing, the transdermal resistance, R_{skin}, dominates the skin impedance. The decrease in R_{skin} following treatment was quantified by the resistance ratio f_R, defined as

$$f_R = \frac{R^i_{skin}}{R^f_{skin}} \qquad (3)$$

Table I. Results of resistance ratio and optical tests[a]

Salicylic acid	Benzoic acid	U_{skin} (V)	τ_{pulse} (ms)	t_{int} (s)	t_{total} (s)	I (mA)	q (mC)	f_R	Macro focus	Micro focus	Vert pool	
Negative controls (n=5): unperturbed skin with PBS in donor								4±1	–	–	–	**Fig 4**
Negative controls (n=5): skin with 70% ethanol in donor								3±1	+	–	–	
Positive controls (n=5)								16±2	+	+	+	**Fig 5**
PBS (n=5)		195	10	3	300	40	40	6±2	–	–	–	**Fig 6†**
70% Ethanol (n=5)		260	5	5	600	60	36	10±1	+	–	–	
0.3%	0.6%	260	5	5	600	64	38	10±1	+	–	–	
3%	6%	237	3.6	5	485	65	22	26	+	+	+	
3%	6%	217	5	5	600	50	30	32	+	+	+	
3%	6%	279	5	5	600	55	33	40	+	+	+	
3%	6%	250	5	5	600	62	37	49	+	+	+	**Fig 7**

[a]Note that in all experiments, following either control exposure, mechanical microhole creation, or electrochemical intervention, the skin was subjected to 1 h iontophoresis at 1 mA per cm^2 (over the area of the microhole in the polyimide sheet) before indicators were ascertained. Four indicators were derived from resistance ratio and optical tests. These are denoted by f_R (resistance ratio), Macro Focus (macroscopic focusing), Micro Focus (microscopic focusing), Vert Pool (vertical pooling), and are described in the text. Some of the results are accompanied by images indexed in the right-hand column. "†" indicates the pulsing only controls (n = 5). Presence/absence of optical indicators are denoted by +/–.

where R^i_{skin} and R^f_{skin} are the initial and final skin resistances, measured before and after the treatment, respectively. The resistances were corrected for a baseline resistance that accounted for the resistance of the PBS between the measuring electrodes and the resistance of the electrodes. The baseline resistance was measured at the end of each experiment with no skin present in the chamber. A large, persisting change in skin resistance was used as an indicator for the creation of a microconduit.

Imaging test To assess the creation of a microconduit, full-thickness skin specimens were first evaluated by imaging using incandescent and fluorescence microscopy. Then, imaging was repeated following heat stripping, and again following treatment with trypsin to confirm the creation of a microconduit.

After the brief electrochemical procedure, the skin specimen was subjected to iontophoresis in the presence of PBS containing sulforhodamine and fluorescent beads. The rationale is that a small, constant current preferentially drives these markers into the low resistance microconduit, thereby marking it identifiable by optical microscopy. On completion of high-voltage pulsing and iontophoresis, the skin was removed from the chamber and rinsed with de-ionized water. The skin was mounted on a microscope slide and examined under a fluorescence microscope (Olympus BH-2, Olympus, Woodbury, NY). The fluorescent image of the skin was acquired using a CCD camera (Pixera, Los Gatos, CA). Imaging was also carried out further at two stages: after heat stripping and (in some cases) after further treatment by enzymatic trypsin digestion. An incandescent (white) light source was placed below the specimen, with observation from above. As light passes through the microconduit, the opening in the skin appears as a single, bright spot surrounded by a dark region of intact skin.

Pressure-driven volumetric flow test The most direct, functional evidence for the presence of a microconduit is a measurable volumetric flow. Thus, a pressure driven flow across the electrochemically treated skin was used as a test for the presence of a microconduit. Either the heat-stripped skin or the enzymatically isolated SC was mounted in the side-by-side chamber (**Fig 3**). Pressure-driven flow was then measured by establishing a hydrostatic pressure difference between the two compartments of the chamber, using a vertical column of up to 12 cm aqueous solution on the donor side. Volumetric flow was measured by recording the height of the solution column meniscus as a function of time, t, and multiplying by the cross-sectional area of the column to obtain the volume accumulation with time.

Well-established fluid dynamics equations (White, 1979) were used to relate the diameter, D_{MC} of the microconduit with the coefficients obtained from the least square fit of a polynomial $a_1t^2 + a_2t$ to the experimental data points for the fluid volume change with time, V(t). The microconduit diameter D_{MC} was calculated assuming fluid flow through an orifice as

$$D_{MC} = \left(\frac{32a_1A_{col}0.6}{g\pi^2}\right)^{1/4} \quad (4)$$

Here, A_{col} is the cross-sectional area of the column of aqueous solution, $g = 9.8$ m per s^2 is the local value of the earth's gravitational acceleration, and 0.6 is the aqueous solution coefficient of velocity for a short tube approximation (White, 1979), which is appropriate for a $\approx 200\,\mu m$ diameter microconduit with a thickness ranging from $\approx 20\,\mu m$ (isolated SC) to $\approx 100 \pm 50\,\mu m$ (heat-stripped skin).

RESULTS AND DISCUSSION

The motivation of this *in vitro* study is to investigate the efficacy of the ethanol, salicylic acid and benzoic acid solution in creating a microconduit in the SC of human skin. The presence of a microconduit was assessed using three independent tests. The results of these tests are summarized in **Tables I** and **II**, and **Figs 4–9**. Based on positive control results, four features were identified as indicators of the presence of a microconduit:

1 f_R, the resistance ratio, which represents the change in skin resistance from the initial, unperturbed state to that following the electrochemical treatment. The presence of a microconduit causes a large increase in f_R.

2 Macro Focus: macroscopic focusing, is the presence of a focused spot on the skin at the site where the microhole of the chamber contacted the skin, as seen in the macroscopic view of the skin. When a microconduit is created using the electrochemical treatment, sulforhodamine present in the donor solution enters the microconduit to form a red fluorescent spot approximately equal in dimension to the microhole in the insulating sheet.

3 Micro Focus: microscopic focusing, is the presence of a focused cluster of negatively charged fluorescent microbeads at the site of the microconduit. If a microconduit is created following the electrochemical treatment, iontophoresis of the skin with highly charged fluorescent beads in the donor compartment causes the beads to be clustered in the microconduit.

4 Vert Pool: vertical pooling, denotes the pooling of the beads throughout the depth of the SC ($\approx 20\,\mu m$) if a microconduit is created in the skin. The vertical pooling of fluorescent beads is determined by acquiring fluorescent images of the skin at various depths.

A large value of f_R accompanied by the presence of the remaining three indicators strongly indicates the presence of a microconduit following the electrochemical procedure. The presence or absence of optical indicators is denoted by + or –, respectively, in **Table I**.

Figures 4–8 display the results of different control and electrochemical treatment procedures on full-thickness human skin. The top left panel shows the macroscopic view of the skin. The top center and top right images are fluorescent images of the skin at different depths (30 μm apart). The bottom panels show fluorescent images of the skin at a higher magnification, acquired at different depths, 5 μm apart.

Negative controls Five negative control experiments were performed on unperturbed full-thickness skin exposed to either

Table II. Results of further imaging and flow tests[a]

Salicylic acid	Benzoic acid	U_{skin} (V)	τ_{pulse} (ms)	t_{int} (s)	t_{total} (s)	I (mA)	q (mC)	f_R	MC visualized	Fluid flow	
3%	6%	249	5	5	600	57	34	43	–	+	
3%	6%	273	5	5	600	61	37	39	–	+	
3%	6%	241	5	5	600	64	38	35	–	+	
3%	6%	299	5	5	600	58	35	42	+	+	
3%	6%	228	5	5	600	60	36	46	+	+	
3%	6%	240	5	5	600	67	40	47	+	+	**Figs 8, 9**

[a]The skin in these experiments was heat stripped and/or treated with trypsin overnight following the electrochemical process of microconduit (MC) creation. The entries in this table are similar to those in **Table I**. Two definite confirmations of a microconduit are listed here for each experiment. MC visualized relates to whether the MC was visualized by optical microscopy, either after heat stripping or treatment with trypsin. Fluid flow indicates whether a fluid flow was observed in the pressure-driven fluid flow test after treatment with trypsin. Presence/absence of definite confirmations are denoted by +/–.

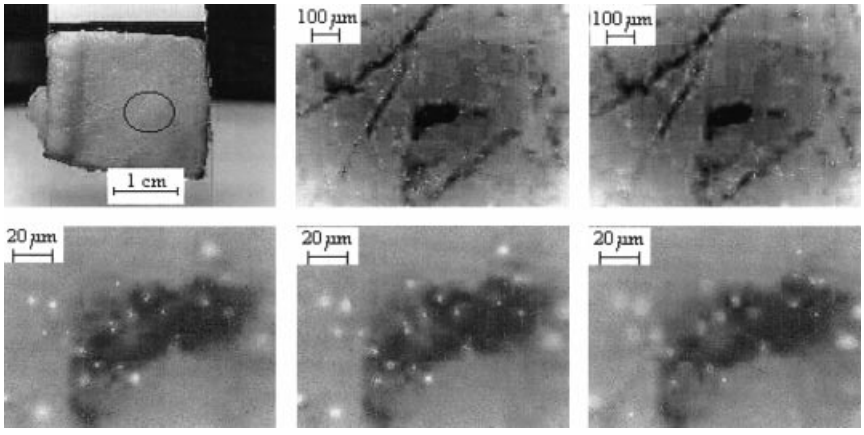

Figure 4. Negative control. A full thickness human skin was subjected only to iontophoresis for 1 h with sulforhodamine and fluorescent beads suspended in saline in the donor compartment. *Top left* is the macroscopic view of the skin. The black ellipse encompasses the site of the polyimide microhole that contacted the skin. No extensive staining of the skin by sulforhodamine is evident. The *top center* and *top right* images are fluorescent images of the skin taken at different depths (30 μm apart). The bright spots, which represent fluorescent beads, indicate discrete binding of beads to the skin. There is no cluster of fluorescent beads present in the skin. The dark region represents staining of the skin by sulforhodamine. The *bottom* images are fluorescent images of the skin at a higher magnification. The images are taken at different depths, 5 μm apart. The disjoint presence of beads is clearly visible. The beads do not persist over a large depth suggesting that there is no pathway spanning the SC in the skin.

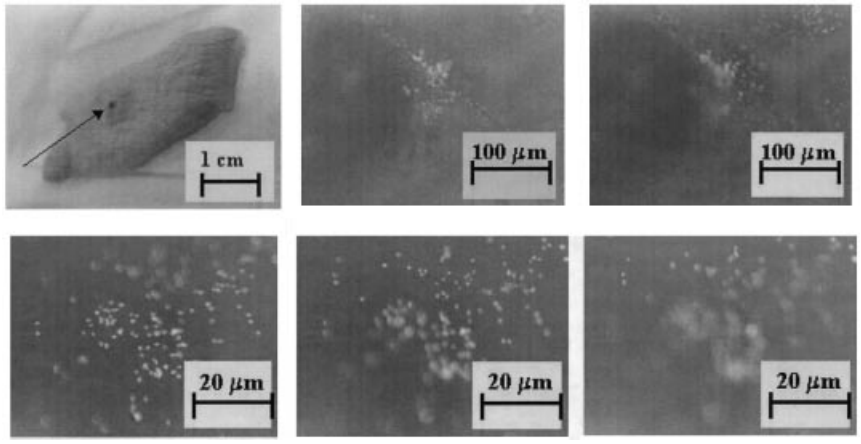

Figure 5. Iontophoresis control. The skin was subjected to iontophoresis for 1 h with Whitfield solution's ingredients in the donor compartment. *Top left* image is the macroscopic view of the skin showing a focused spot stained by sulforhodamine. The *top center* and *top right* images are fluorescent images of the skin taken at different depths (30 μm apart). The bright spots, which represent fluorescent beads, indicate only discrete binding of beads to the skin. There is no cluster of fluorescent beads present in the skin. The dark region represents staining of the skin by sulforhodamine. The *bottom* images are fluorescent images of the skin at a higher magnification. The images are taken at different depths, 5 μm apart. The disjoint presence of beads is clearly visible suggesting that there is microconduit in the skin.

PBS only or to 70% ethanol and 30% PBS. The skin was subjected to iontophoresis in the presence of the fluorescent markers for the same duration as in an experiment with electrochemical treatment. The resistance ratio was 4 ± 1 (PBS only) and 3 ± 1 (70% ethanol and 30% PBS) following iontophoresis (**Table I**). Iontophoresis of unperturbed skin did not cause a focused clustering of beads at the site of the microhole and the beads did not persist throughout the depth of SC (**Fig 4**), i.e., Micro Focus and Vert Pool were negative, respectively. The macroscopic view of the skin did not show a focused spot where the skin contacted the microhole in the polyimide sheet, when exposed to PBS only. When exposed to 70% ethanol, Macro Focus was positive, indicating minor perturbation of lipids of SC, allowing binding of sulforhodamine.

Iontophoresis controls Five iontophoresis control experiments were performed on full-thickness skin exposed to 1 h of 1 mA per cm^2 iontophoresis in the presence of salicylic acid and benzoic acid. The resistance ratio following the treatment was 4 ± 2 (**Table I**).

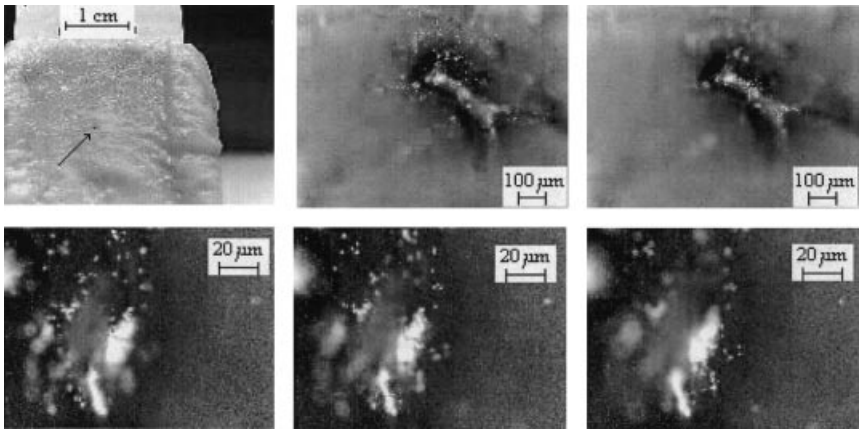

Figure 6. Positive control. A shallow ≈200 μm hole was drilled into the full-thickness skin using a cobalt microprecision drill. The skin was then subjected to iontophoresis for 1 h in the presence of sulforhodamine and latex beads suspended in PBS in the donor compartment. The *top left* image shows the macroscopic view of the image following iontophoresis. A focused red (here dark) spot (denoted Macro Focus in **Table I**) is seen (*arrow*) at the site where the skin came into contact with the microhole in the chamber. *Top center* and *top right* images are fluorescent images of the skin, imaged 20 μm apart in depth. The images show a dense cluster of fluorescent beads at the site of the microhole (denoted Micro Focus in **Table I**). Images in the *bottom panel* show the fluorescent images at a higher magnification, separated by 15 μm in depth. The cluster of fluorescent beads persists over more than 15 μm in depth (denoted Vert Pool in **Table I**). Contrast to the negative control experiments, the beads are not distributed as individual beads, they are instead clustered within the microhole.

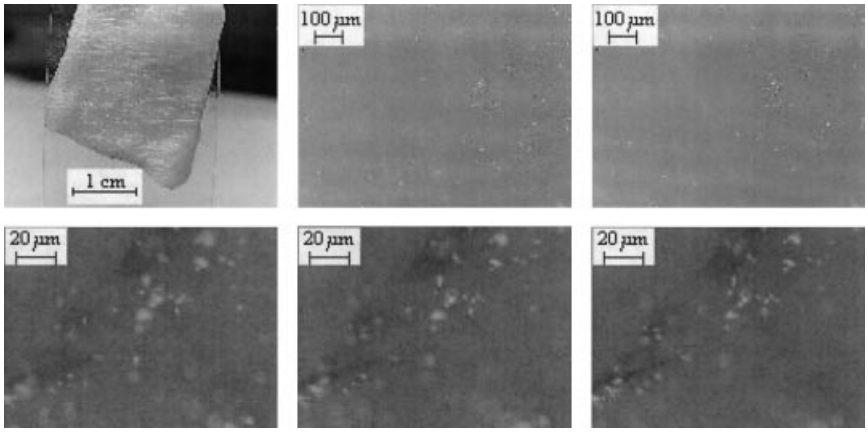

Figure 7. Pulsing control. A full-thickness skin specimen was subjected to high-voltage pulsing and iontophoresis (**Table I**, third row) with only PBS and fluorescent markers in the donor compartment during high-voltage pulsing and iontophoresis, respectively. *Top left* image (macroscopic view) shows no focused red spot. The low-magnification fluorescent images (*top center* and *top right*; 30 μm apart in depth) show no areas with large density of fluorescent beads. Similarly, the magnified fluorescent images (*bottom panel*, 5 μm apart in depth) show only a scattered, distribution of fluorescent beads. These images suggest that there was no extensive keratin disruption following high-voltage pulsing when keratolytic agents were absent during high-voltage pulsing.

Following the treatment, the skin was subjected to another 1 h of iontophoresis with the fluorescent dye solution in the donor chamber. Iontophoresis of unperturbed skin did not cause a focused clustering of beads at the site of the microhole and the beads did not persist throughout the depth of SC (**Fig 5**), i.e., Micro Focus and Vert Pool were negative, respectively; however, the macroscopic view of the skin showed a focused spot where the skin contacted the microhole in the polyimide sheet (**Fig 5**). It is clear that iontophoresis treatment alone is not sufficient to transport the keratolytic molecules into the corneocytes to create a microconduit in the skin.

Positive controls In five positive control experiments, an approximately 200 μm diameter hole through the SC and about 40 ± 20 μm deep was created by a cobalt microprecision drill bit in full-thickness human cadaver skin. The skin specimen was then subjected to iontophoresis with PBS containing fluorescent markers in the donor compartment (contacting the SC). Following the creation of a hole in the skin, f_R was 16 ± 2, indicating the presence of new aqueous pathways in the skin. In addition, all three optical indicators were present (**Table I**). A well-defined spot was visible in the skin, stained red (fluorescence) by sulforhodamine in the donor solution (**Fig 6**, top left; this represents Macro Focus). The fluorescence image of the skin also revealed a dense cluster of fluorescent beads in the spot (**Fig 6**, top right; this represents Micro Focus). The cluster of beads persisted as the plane of view was moved deeper than 15 μm from the SC surface (**Fig 6**, bottom; this represents Vert Pool). The small, constant iontophoresis current preferentially had driven the beads into the low resistance microhole.

Pulsing control Two types of pulsing controls were performed. In the first case, the donor compartment contained PBS whereas in the second case, the donor compartment contained 70% ethanol in PBS. In both cases, the skin was subjected to high-voltage pulsing and iontophoresis, but without any keratolytic molecules in the donor solution.

When the skin was pulsed in the presence of PBS, with 40 mC of charge delivered, the resistance ratio increased to 6, similar to an increase to 4 in the negative control experiments (**Table I**). As in the negative control experiments, all three optical indicators were negative. The fluorescence image of the skin showed no areas with clustered beads, only scattered beads were visible (**Fig 7**). These indicators suggest that high-voltage pulsing alone causes no disruption to the keratin matrix and therefore does not create a microconduit in the SC.

When the skin was pulsed in 70% ethanol, the resistance ratio increased to 10 ± 1 when the total charge delivered was 36 mC. The macroscopic view of the skin showed a focused red spot at the site of the microhole. The other two fluorescent indicators were negative. The presence of ethanol during high-voltage pulsing only marginally increased the permeability of SC and thus the appearance of a sulforhodamine-stained spot on the skin due to increased access to lipids.

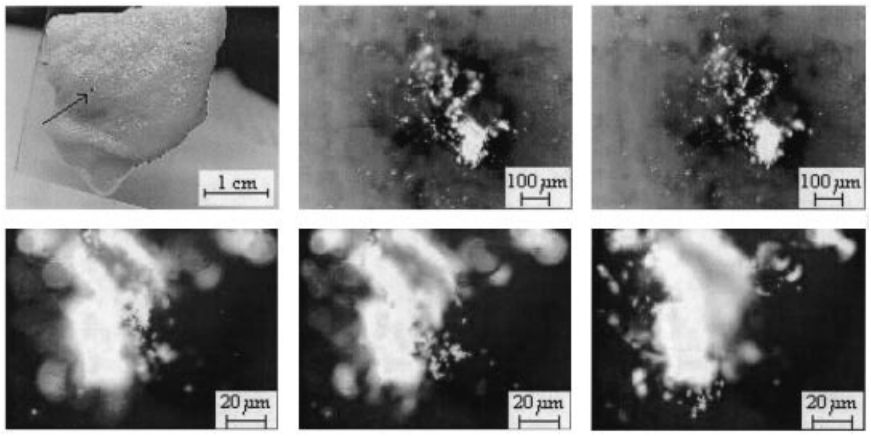

Figure 8. Electrochemical creation of a microconduit. A full-thickness skin specimen was subjected to a 10 min electrochemical treatment involving 3% salicylic acid and 6% benzoic acid in 70% ethanol and 30% PBS (**Table I**). The electrochemical protocol is followed by iontophoresis for 1 h at 1 mA per cm^2 in the presence of large latex beads and sulforhodamine. The macroscopic view of the skin (*top left*) shows a focused red spot at the site of microhole contact. The fluorescent images (*top center* and *top right*; 20 μm apart in depth) show a dense cluster of fluorescent beads. The fluorescent images at higher magnification (*bottom panel*; 15 μm depth intervals) also show a cluster of beads that persist over 20 μm deep. These images relate to positive indicators, labeled Macro Focus, Micro Focus, and Vert Pool in **Table I**. The features in these images are essentially the same as those obtained in positive control experiments (**Fig 5**). The results suggest that a SC-spanning microhole has been created in the full-thickness skin following electrochemical treatment.

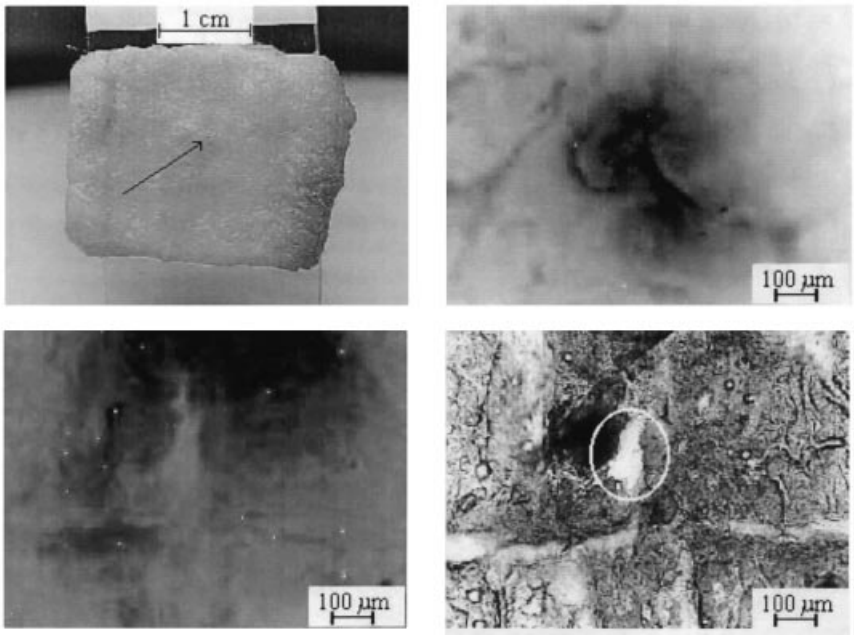

Figure 9. Visualization of a microconduit. A full-thickness skin was subjected to a 10 min electrochemical process (**Table II**) in the presence of sulforhodamine. *Top left* image shows the macroscopic view of the skin, with a focused red (here dark) spot formed by sulforhodamine staining of the microconduit (*arrow*). *Top right* is the corresponding fluorescent image, which shows the presence of sulforhodamine in the microconduit (seen as dark regions in the gray-scale image). The skin was then heat stripped to get a thinned specimen. *Bottom left* shows the fluorescent image of the heat-stripped skin. The central bright region is the region of the skin that contacted the microhole in the polyimide sheet. The *bottom right* is an incandescent image of the heat-stripped skin, illuminated from below using a bright light source. The microconduit in the skin (enclosed by the white circle) is brightly illuminated by light passing through the microconduit in the skin. This image provides the most striking optical evidence of the presence of a microconduit in the skin.

Electrochemical creation of a microconduit The main objective of this study is to characterize the use of high-voltage pulsing and two pathway-enlarging molecules to create a microconduit in human skin. The parameters of high-voltage pulsing and concentrations of the keratolytic chemicals were varied to optimize the process of microconduit creation.

Pulsing control experiments demonstrated that high-voltage pulsing alone does not disrupt the keratin matrix. Salicylic acid and benzoic acid are present in concentrations of 3% and 6% in Whitfield's solution. Electrochemical treatment of full-thickness skin with 1/10th this concentration did not reveal the presence of a microconduit. Only one of three optical indicators was positive (**Table I**). Although the skin showed a macroscopic red spot indicating sulforhodamine staining of the ethanol altered lipids, no cluster of fluorescent beads was found in the red spot. Following the treatment, f_R increased to $\approx 10 \pm 1$, less than that observed in positive control experiments. This suggests that the concentrations of the keratolytic components were not high enough to cause an enlarged pathway in SC.

As a low concentration of keratolytic agents did not enlarge pathways created by high-voltage pulsing, the remaining experiments were conducted at concentrations present in Whitfield's ointment. Thus, during the electrochemical intervention, the donor compartment contained 3% salicylic acid and 6% benzoic acid in 70% ethanol with two fluorescent markers. The results of these experiments are tabulated in the last four rows of **Table I**.

Electrochemical treatment of full-thickness human skin with 3% salicylic acid and 6% benzoic acid consistently created a microconduit in SC. This was ascertained from resistance ratio and imaging tests. All three imaging indicators were positive in these experiments. The resistance ratio, following electrochemical intervention, ranged from 26 to 49 (**Table I**, last four rows). These values are higher than even that measured in positive control experiments. This strongly supports the presence of an enlarged aqueous pathway in the treated skin.

Figure 8 shows the images of a full-thickness skin specimen following electrochemical treatment. In the macroscopic view (top left), a well-defined red spot is clearly seen at the site where the skin contacted the microhole in the polyimide sheet. The red spot

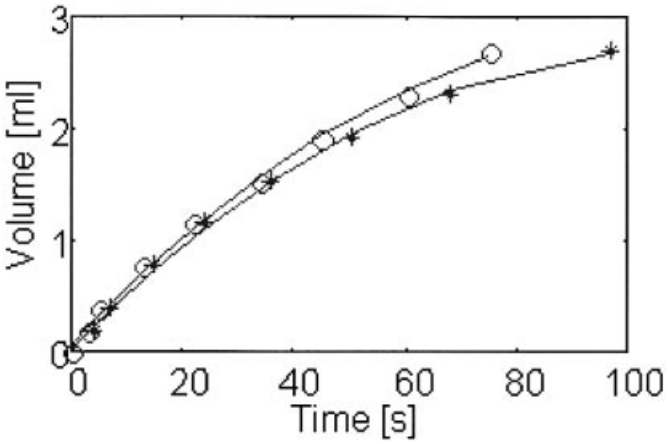

Figure 10. Volume *vs* time due to pressure-driven volumetric flow through a microconduit. The heat-stripped skin of **Fig 8** was treated with trypsin overnight to obtain an isolated SC preparation. The skin was mounted in the side-by-side chamber with a hydrostatic pressure column (**Fig 2**). The pressure difference caused a flow through the microconduit in the skin. The decrease in the aqueous column height was recorded as a function of time (indicated by ○ and * for two independent data sets). A theoretical fit to the flow data (Eq 4) is shown by the solid line, yielding a microconduit diameter of $200 \pm 20\,\mu m$.

results from the staining of sulforhodamine, which now finds access to corneocytes deeper into the skin (Macro Focus positive). The fluorescence images of the skin (top center and top right) show a dense cluster of fluorescent beads in the microconduit (Micro Focus positive). Iontophoresis following the microconduit creation phase of the protocol concentrates the charged beads at the site of the lowest resistance, i.e., the microconduit. The fluorescence images of the skin at a higher magnification (bottom panels) show that the cluster of fluorescent beads persists over $20\,\mu m$ in depth from the surface of the SC (Vert Pool positive). This provides strong evidence that a microconduit has been created that spans the SC following treatment with the keratolytic chemicals.

Direct comparison of the results associated with an electrochemically created microconduit using indicators observed in ''positive controls'' were used to establish tentative conditions for microconduit creation; however, the degree of keratin disruption is not easily ascertained using these indicators. Hence in the next six experiments listed in **Table II**, the full-thickness skin was thinned after electrochemical treatment either by heat stripping alone or by treating the heat-stripped skin with trypsin. Imaging and flow tests on thinned skin provided confirmatory evidence of the presence of a microconduit (**Figs 9** and **10**).

In **Fig 9**, the top panels (left and right) show macroscopic and microscopic views of the sulforhodamine-stained skin after the electrochemical protocol. The bottom images were acquired after skin thinning. The heat-stripped skin shows a red spot (the light gray region in **Fig 9**, bottom left) at the site of microhole indicating the sulforhodamine staining of the region exposed to the electrochemical treatment. When heat-stripped skin is exposed to incandescent light from below, a bright region is seen at the site of the microconduit (**Fig 9**, bottom right). This provides a strong evidence that a microconduit spanning the SC has been created, which allows light to pass through.

More striking evidence of a microconduit is provided by the flow tests on skin treated with trypsin following the electrochemical treatment. Treatment with trypsin leaves mostly the SC, therefore a microconduit spanning the SC should support a measurable flow. Pressure-driven flow was measured by establishing a small hydrostatic pressure difference between the two compartments of the chamber, using a vertical column of up to 12 cm aqueous solution on the donor side. **Figure 10** shows the volume of solute transported through the microconduit as a function of time. The measured flow was compared with fit to theoretical model (Eqn 4) to estimate the size of the microconduit. The best fit estimate for the microconduit diameter of the specimen shown is $200 \pm 20\,\mu m$. This dimension, along with the resistance ratio values and other four indicators, is similar to that observed in positive control experiments.

The striking confirmatory evidence for the presence of a microconduit was obtained from the volumetric flow test. Fluid flow was consistently observed in all six different electrochemical treatments (**Table II**), even in the isolated SC cases where microconduit could not be directly visualized (microconduit visualized negative). The heat-stripping procedure leaves a variable number of epithelial layers attached to the SC, which prevents light from passing through a microconduit spanning only the SC. Treatment with trypsin removed the epithelium, leaving only the SC; however, the resulting preparation is too thin to provide an optical contrast between the microconduit and the rest of the intact SC. In such conditions, a microconduit is difficult to visualize directly. A pressure-driven flow alone provides reliable evidence for the presence of a microconduit. The flow test indicates that the electrochemical procedure used in this study creates microconduits in the range of $200\,\mu m$, which support fluid transport in the order of 0.01 ml per s.

Keratolytic molecules Previous experiments (Zewert *et al*, 1999) using STS showed that a macromolecule (lactalbumin, $\approx 15{,}000$ g per mol) and $\approx 1\,\mu m$ charged beads were transported through microconduits in heat-stripped skin; however, a large variability in microconduit creation was observed in these experiments. A following study (Ilic *et al*, 1999) employed STS with urea to achieve a more controlled microconduit creation. The use of urea as an alkylating agent prevented the oxidation of disulfide bridges reduced by STS. In this study, another solution known for its keratolytic potential was used to create microconduits.

Both salicylic acid and benzoic acid are small, and are easily introduced into corneocytes by electroporation. high-voltage transdermal voltage pulses create new, small aqueous pathways (''pores'') in the multilamellar lipids of the SC, thereby providing salicylic acid and benzoic acid with entry points into corneocytes. During pulsing, these chemicals are electrically driven into corneocytes within a local transport region. Salicylic acid degrades the keratin within electroporated corneocytes, thereby greatly decreasing the steric hindrance over the localized area of the skin exposed to the chemicals and high-voltage pulses (**Fig 1**). This results in a greatly enlarged aqueous pathway, namely, a microconduit spanning the SC. In this study, partially optimized protocol lasting about 5 min was needed to create a microconduit.

Salicylic acid is routinely used to degrade and extract keratin. Salicylic acid and benzoic acid, active ingredients of Whitfield's solution, achieve the chemical decomposition of keratin by breaking the keratin peptide bonds and by reducing the binding forces within the SC and find wide applications in treatment of skin ailments. In our protocol, the skin is exposed to a small amount of salicylic acid and benzoic acid over a microscopic region for less than 5 min. This level of exposure is considerably lower than that in established applications of Whitfield's ointment. Hence, we expect no toxic effects to result from the electrochemical treatment reported here.

Localization of SC disruption An insulating sheet with a microhole was used in contact with the SC to limit the electrochemical intervention to a very small area of the skin. As shown previously, even without a perfect seal, such a masking causes localized electroporation at the microholes (Gowrishankar *et al*, 1999). Electrochemical treatment through a $200\,\mu m$ microhole in the polyimide sheet was shown to create a $200 \pm 20\,\mu m$ diameter microconduits spanning the SC. A simple extension of this result suggests that a reduction in the size of the masking microhole would result in a smaller microconduit.

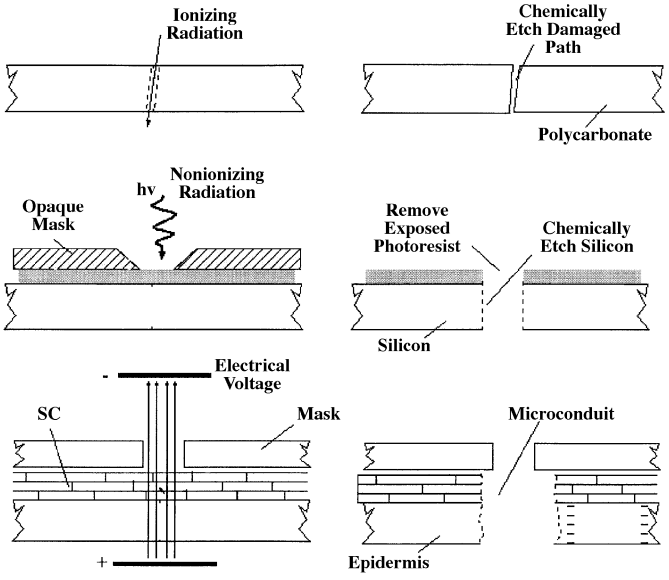

Figure 11. Comparison of established and microconduit microfabrication methods. The common basic idea is that of a localized physical perturbation followed by chemical (keratolytic agent) disruption of a local region made accessible by the physical perturbation. *Top*: Creation of a track-etched filter (e.g., Nucleopore) by ionizing radiation and subsequent chemical etch. *Center*: Semiconductor photolithography using localized light exposure followed by chemical removal of exposed silicon regions. *Bottom*: Microconduit creation by localized SC electroporation followed by chemical disruption of the now accessible material (keratin matrix and apparently corneocyte envelopes) within corneocytes.

Aqueous pathway creation time The protocol used in this study provides a reliable creation of a microconduit with a 10 min ($t_{total} = 600$ s) electrochemical intervention; however, the cumulative electrical exposure is much shorter, less than 1 s. If only an electrical exposure in the presence of the keratolytic molecules is needed to create a microconduit, the present protocol might be shortened to a very rapid (less than 1 s) procedure; however, the role of the extra incubating period of the irreversible degradation of the keratin matrix is not yet established.

Microfabrication of transdermal aqueous pathways Miniature devices that interface with biologic systems over a microscopic area are being designed both for drug delivery and sensing. Systems based on gas generation by an electrolytic reaction (O'Keefe *et al*, 1994) and on a shape memory actuated microvalve system (Reynaerts *et al*, 1996) have been developed and tested for liquid drug delivery. A Microelectromechanical system for drug delivery using iontophoresis has been reported recently (Wouters and Dinh, 1997). Of late, there has also been an increasing interest in flow type biosensing devices, which take up samples at a constant rate and perform an *in situ* or *in vivo* monitoring (Steenkiste *et al*, 1997). Our study provides a method for rapidly microengineering a pathway in the skin to interface future devices for delivery and sampling of biologically relevant fluids.

Localized physical perturbations One classic example is track-etched filter fabrication (Nucleopore), in which penetrating ionizing particles create a damage track through a polycarbonate thin sheet, followed by chemical etching along the damage track. Another is the widespread use of photolithography in semiconductor fabrication, where physical masks control which regions are exposed to various kinds of light, and after selected regions experience photodamage to material such as photoresist, a chemical etch removes material from targeted regions. We view the *in situ* creation of a microconduit as an analogous process: localized high-voltage pulsing creates localized aqueous pathways, through which keratolytic ions or molecules are introduced, leading to selective removal of material to create a microconduit. This analogy is illustrated in **Fig 11**.

The creation of a SC-spanning microconduit that encompasses a microscopic area of the skin may enable the miniaturization of all the elements of a transdermal drug delivery system while providing an acceptable level of transport. A spatially localized intervention may lead to acceptable levels of sensation and unobtrusiveness, which are essential for the widespread application of a medical system.

We thank J. Howard for preparing the perforated polyimide films. We also thank B. Mikic, E. A. Gift, and T. Chen for technical support and stimulating discussions. This work was supported by the National Institutes of Health, Grant RO1-ARH4921, the Whitaker Foundation, Grant RR10963, and a grant from the MIT Lincoln Laboratory Advanced Concepts Committee.

REFERENCES

Anderson BD, Higuchi WI, Raykar PV: Heterogeneity effects on permeability partition–coefficient relationships in human stratum corneum. *Pharm Res* 5:566–573, 1988

Bennett JE: Miscellaneous mycoses and *Prototheca* infections. In *Harrison's Principles of Internal Medicine*, 14th edn. New York: McGraw-Hill, 1998, pp 1158–1161

Bergstresser PR, Chapman SL: Maturation of normal human epidermis without an ordered structure. *Br J Dermatol* 102:641–648, 1980

Budavari S (ed.): *The Merck Index*, 12th edn. Rahway: Merck and Co, 1996

Chen T, Segall EM, Langer R, Weaver JC: Skin electroporation: Rapid measurements of the transdermal voltage and flux of four fluorescent molecules show a transition to large fluxes near 50 V for 1 ms pulses. *J Pharm Sci* 87:1368–1374, 1998

Chen T, Langer R, Weaver JC: Charged microbeads are not transported across human stratum corneum *in vitro* by short high-voltage pulses. *Bioelectrochem Bioenerg* 48:181–192, 1999

Clayton YM, Connor BL: Comparison of clotrimazole cream, Whitfield's ointment and nystatin ointment for the topical treatment of ringworm infections, pityriasis versicolor, erythrasma and candidiasis. *Br J Dermatol* 89:297–303, 1973

Degano P, Sarphie DF, Bangham CRM: Intradermal DNA immunization of mice against influenza a virus using the novel PowderJect(R) system. *Vaccine* 16:394–398, 1998

Diehl KB: Topical antifungal agents: an update. *Am Fam Phys* 54:1687–1692, 1996

Eppstein JA, Delcher HK, McRae MS: A clinical feasibility study for the transdermal delivery of parathyroid hormone 1–34 through MicroPors™. *Proc Int Symp Control Rel Bioact Mater, Controlled Release Society* 26:409, 1999

Gloor M, Beier B: Keratoplastic effect of salicylic acid, sulfur and a tensio-active mixture. *Z Hautkr* 59:1657–1660, 1984

Gooskens V, Pönnighaus JM, Clayton Y, Mkandawire P, Sterne JA: Treatment of superficial mycoses in the tropics: Whitfield's ointment versus clotrimazole. *Int J Dermatol* 33:738–742, 1994

Gowrishankar TR, Herndon TO, Vaughan TE, Weaver JC: Spatially constrained localized transport regions due to skin electroporation. *J Contr Rel* 60:101–110, 1999

Gummer CL: The in vitro evaluation on transdermal delivery. *Transdermal Drug Delivery: Developmental Issues and Research Initiatives*. New York. Marcel Dekker, 1989, pp 177–186

Guy RH: Current status and future prospects of transdermal drug delivery. *Pharm Res* 13:1765–1768, 1996

Henry S, McAllister DV, Allen MG, Prausnitz MR: Microfabricated microneedles: a novel approach to transdermal drug delivery. *J Pharm Sci* 87:922–925, 1998

Holti G: A double-blind controlled trial of Whitfield's ointment and variotin in ringworm infections with a two year follow-up. *Acta Derm Venerol* 50:229–231, 1970

Huber C, Christopher E: Keratolytic effect of salicylic acid. *Arch Dermatol Res* 257:293–297, 1977

Ilic L, Gowrishankar TR, Vaughan TE, Herndon TO, Weaver JC: Spatially constrained skin electroporation with sodium thiosulfate and urea creates transdermal microconduits. *J Contr Rel* 61:185–202, 1999

Kost J, Mitragotri S, Gabbay RA, Pishko M, Langer R: Transdermal monitoring of glucose and other analytes using ultrasound. *Nat Med* 6:347–350, 2000

Langer R: Drug delivery and targeting. *Nature* 392:S5–S10, 1998

Lee S, McAuliffe DJ, Flotte TJ, Kollias N, Doukas AG: Photomechanical transcutaneous delivery of macromolecules. *J Invest Dermatol* 111:925–929, 1998

Lin AN, Nakatsui T: Salicylic acid revisited. *Int J Dermatol* 37:335–342, 1998

Lin LW, Pisano AP: Silicon-processed microneedles. *J Microelectromechan Syst* 8:78–84, 1999

Lóden M, Boström P, Kneczke M: Distribution and keratolytic effect of salicylic acid and urea in human skin. *Skin Pharmacol* 8:173–178, 1995

Menton DN: A minimum-surface mechanism to account for the organization of cells into columns in the mammalian epidermis. *Am J Anat* 145:1–22, 1976

Merino V, Kalia YN, Guy RH: Transdermal therapy and diagnosis by iontophoresis. *Trends Biotechnol* 15:288–290, 1997

Mitragotri S, Blankschtein D, Langer R: Ultrasound-mediated transdermal protein delivery. *Science* 269:850–853, 1995

Nelson JS, McCullough JL, Glenn TC, Wright WH, Lia LHLW, Jacques S: Midinfrared laser ablation of stratum-corneum enhances *in vitro* percutaneous transport of drugs. *J Invest Dermatol* 97:874–879, 1991

Neubert R, Partyka D, Wohlrab W, Dettlaff B, Fürst W, Taube KM: Penetration of salicylic acid and salicylate into the multilayer system and into the human horny layer. *Dermatol Monatsschr* 176:711–716, 1990

Nook TH: *In vivo* measurement of keratolytic effect of salicylic acid in three ointment formulations. *Br J Dermatol* 117:243–245, 1987

O'Keefe D, O'Herlihy C, Gross Y, Kelly JG: Patient-controlled analgesia using a miniature electrochemically driven infusion pump. *Br J Anaesth* 73:843–846, 1994

Pliquett U: Mechanistics of molecular transdermal transport due to skin electroporation. *Adv Drug Deliv Rev* 35:41–60, 1999

Pliquett UF, Gusbeth CA, Weaver JC: Non-linearity of molecular transport through human skin due to electric stimulus. *J Contr Rel* 68:373–386, 2000

Reynaerts D, Peirs J, Van Brussel H: A SMA-actuated implantable system for delivery of liquid drugs. In: Borgmann H, ed. *Proceedings of Actuator '96, Bremen, Germany*, Germany: Tech Consult GmbH, 1996, pp 379–382

Russell D, Russell AD: Treatment of ringworm—old remedy vs new. *J Infect* 24:333, 1992

Schaefer H, Redelmeier TE: *Skin Barrier: Principles of Percutaneous Absorption*. Basel: Karger, 1996

Smith A, Yang D, Delcher H, Eppstein J, Williams D, Wilkes S: Fluorescein kinetics in interstitial fluid harvested from diabetic skin during fluorescein angiography: Implications for glucose monitoring. *Diabetes Tech Ther* 1:21, 1999

Smith EW, Maibach HI (eds): *Percutaneous Penetration Enhancers* Boca Raton: CRC Press, 1995

Steenkiste FV, Baert K, Debruyker D, *et al*: A microsensor array for biochemical sensing. *Sensors Actuators* B 44:409, 1997

Tamada JA, Bomannon NJV, Potts RO: Measurement of glucose in diabetic subjects using noninvasive transdermal extraction. *Nature Med* 1:1198–1202, 1995

Weaver JC, Chizmadzhev YA: Theory of electroporation: a review. *Bioelectrochem Bioenerg* 41:135–160, 1996

Weaver JC, Vanbever R, Vaughan TE, Prausnitz MR: Heparin alters transdermal transport associated with electroporation. *Biochem Biophys Res Commun* 234:637–640, 1997

Weaver JC, Vaughan TE, Chizmadzhev Y: Theory of skin electroporation: Implications of straight-through aqueous pathway segments that connect adjacent corneocytes. *J Invest Dermatol Symp Proc* 3:143–147, 1998

Weaver JC, Vaughan TE, Chizmadzhev YA: Theory of electrical creation of aqueous pathways across skin transport barriers. *Adv Drug Del Rev* 35:21–39, 1999a

Weaver JC, Zewert TE, Pliquett UF, *et al*: Pathway-enlarging molecules for skin electroporation: The possibility of macromolecule delivery with minimal side effects. *Proceedings of the 6th Conference on Perspectives in Percutaneous Penetration,* Cardiff: STS Publishing, 1999b

White FM: *Fluid Mechanics*. New York: McGraw-Hill, 1979

Wouters SE, Dinh SM: Microelectrochemical systems for drug delivery. *Electrochim Acta* 42:3385–3390, 1997

Wright S, Robertson VJ: An institutional survey of tinea capitis in Harare, Zimbabwe and a trial of miconazole cream versus Whitfield's ointment in its treatment. *Clin Exp Dermatol* 11:371–377, 1986

Wu JR, Chappelow J, Yang J, Weimann L: Defects generated in human stratum corneum specimens by ultrasound. *Ultrasound Med Biol* 24:705–710, 1998

Zewert TE, Pliquett UF, Langer R, Weaver JC: Transport of DNA antisense oligonucleotides across human skin by electroporation. *Biochem Biophys Res Commun* 212:286–292, 1995

Zewert TE, Pliquett U, Vanbever R, Langer R, Weaver JC: Creation of transdermal pathways for macromolecule transport by skin electroporation and a low toxicity, pathway-enlarging molecule. *Bioelectrochem Bioenerget* 49:11–20, 1999